The polycomb group protein PCGF6 mediates germline gene silencing by recruiting histone-modifying proteins to target gene promoters

Received for publication, November 29, 2019, and in revised form, May 27, 2020 Published, Papers in Press, June 1, 2020, DOI 10.1074/jbc.RA119.012121

Mengjie Liu[1], Yaru Zhu[1], Fei Xing[2], Shuang Liu[1], Yin Xia[3], Qing Jiang[4], and Jinzhong Qin[1,*]

From the [1]State Key Laboratory of Pharmaceutical Biotechnology and MOE Key Laboratory of Model Animals for Disease Study, Model Animal Research Center, Nanjing University, Nanjing, China, the [2]College of Animal Science and Technology, Nanjing Agricultural University, Nanjing, China, the [3]School of Biomedical Sciences, Chinese University of Hong Kong, Hong Kong, China, and the [4]Department of Sports Medicine and Adult Reconstructive Surgery, Nanjing Drum Tower Hospital Affiliated to Medical School of Nanjing University, Nanjing, China

Edited by Qi-Qun Tang

Polycomb group (PcG) proteins are essential for maintenance of lineage fidelity by coordinating developmental gene expression programs. Polycomb group ring finger 6 (PCGF6) has been previously reported to repress expression of lineage-specific genes, especially germ cell–related genes in mouse embryonic stem cells (ESCs) via the noncanonical polycomb repressive complex PRC1.6. However, the molecular mechanism of this repression remains largely unknown. Here, using RNA-Seq, real-time RT-PCR, immunohistochemistry, immunoprecipitation, and ChIP analyses, we demonstrate that PCGF6 plays an essential role in embryonic development, indicated by the partially penetrant embryonic lethality in homozygous PCGF6 (*Pcgf6*$^{-/-}$)-deficient mice. We also found that surviving *Pcgf6*-deficient mice exhibit reduced fertility. Using the *Pcgf6*-deficient mice, we observed that ablation of *Pcgf6* in somatic tissues robustly derepresses germ cell–related genes. We further provide evidence that these genes are direct targets of PCGF6 in ESCs and that endogenous PCGF6 co-localizes with the histone-modifying proteins G9A histone methyltransferase (G9A)/G9a-like protein (GLP) and histone deacetylase 1/2 (HDAC1/2) on the promoters of the germ cell–related genes. Moreover, the binding of these proteins to their target genes correlated with methylation of Lys-9 of histone 3 and with the status of histone acetylation at these genes. Moreover, the recruitment of G9A/GLP and HDAC1/2 to target promoters depended on the binding of PCGF6. Our findings indicate that PCGF6 has a critical role in safeguarding lineage decisions and in preventing aberrant expression of germ cell–related genes.

PcG proteins act as evolutionarily conserved epigenetic mediators of transcription that have integral roles in stem cell identity and development by repressing key developmental genes (1–3). PcG proteins are categorized into at least two biochemically and functionally distinct multisubunit complexes, the polycomb repressive complex 1 (PRC1) and 2 (PRC2), which deposit monoubiquitination of histone H2A at Lys-119 (H2AK119ub1) and trimethylation at lysine 27 of histone H3 (H3K27me3), respectively (1, 2). In mammals, the PRC2 complex comprises the catalytic subunits Ezh1/Ezh2 and their interacting partners Eed and Suz12 (4). The canonical PRC1 complex comprises four core subunits: RING E3 ligase (Ring1A/B), Pcgf (Pcgf1–6), Cbx (polycomb; Cbx2/4/6/7/8), and Phc (polyhomeotic homologues; Phc1/2/3) (1, 2, 5). In noncanonical PRC1 complexes, Cbx and Phc proteins are replaced by Rybp/Yaf2 (5). Importantly, based on the exclusive association of one of the six Pcgf protein homologues, there exist six functionally distinct groups of mammalian PRC1 complexes named PRC1.1–1.6 (6).

PCGF6 was initially identified in a multimeric complex associated with the E2F6 transcription factor in HeLa cells, termed E2F6.com, that contains E2F6, DP1, MAX, MGA, L3MBTL2, RING1A/B, PCGF6, CBX3, YAF2, G9A (also known as EHMT2: euchromatic histone lysine *N*-methyltransferase 2), and GLP (G9A-like protein 1, also known as EHMT1) (7). Subsequent studies in other cell types, including ESCs (8), demonstrate that the major E2F6.com resembles PRC1.6 complex (6, 9). Essential roles for Pcgf6 in maintenance of ESC state has been demonstrated (10–12). *Pcgf6* was identified as an essential self-renewal gene in ESCs by an unbiased genome-wide RNAi screen (13). More recent knockout studies revealed that Pcgf6 is required for ESC identity (10, 12). Notably, the transcriptional profile of *Pcgf6*-null ESCs, examined by microarray analysis or RNA-Seq, revealed the comprehensive repression of germline-specific genes by Pcgf6 (10, 12). Of interest, the expression of germ cell–specific genes is globally repressed in ESCs and all somatic cells in the body. Failure to appropriately express these genes in meiotic cells often results in a partial or complete loss of fertility (14), whereas illegitimate expression in somatic cells may lead to catastrophic consequences such as oncogenic transformation (15). However, the mechanisms that govern Pcgf6-mediated timely silencing of the germline-specific genes remain poorly understood. Intriguingly, the association of Pcgf6 with G9a/Glp (7), with major euchromatic H3K9me1 and H3K9me2 HKMTs (histone lysine methyltransferases), and with the histone deacetylase Hdac1/2 suggests that epigenetic modulations could play a role in silencing of germ line–expressed genes (8). Unfortunately, this issue has not been addressed experimentally.

In this study, we showed that disruption of the *Pcgf6* gene led to partial embryonic lethality, and mutant male and female mice

This article contains supporting information.

* For correspondence: Jinzhong Qin, qinjz@nicemice.cn.

exhibited significantly impaired fertility. In the surviving *Pcgf6*-deficient mice, Pcgf6 was found to be essential for silencing germ cell–specific genes in somatic tissues, thereby suppressing the germ cell differentiation program. Furthermore, G9a/Glp and Hdac1/2 existed in a repressive complex assembled by Pcgf6. Pcgf6 directly bound to its silenced genes, and its binding highly correlated with G9a/Glp and Hdac1/2 in ESCs. Moreover, deletion of the *Pcgf6* gene induced robust reduction of H3K9me1/2, accompanied with derepression of germ cell–specific genes. Our data genetically demonstrate mechanistic insight into how Pcgf6 acts as a dedicated repressor of genes associated with meiosis and germ cells, thereby preserving the identity of ESCs as well as somatic cells under physiological conditions.

Results

Pcgf6 null mice display partially penetrant embryonic lethality

To uncover the biological role of *Pcgf6 in vivo*, we generated mice with targeted disruption of the *Pcgf6* locus (Fig. 1*A*). The conserved RING motif is located in exon 3 of the *Pcgf6* gene (16); therefore, we designed a conditional targeting construct spanning 2 kb to disrupt exons 2, 3, 4, and 5. A loxP site (3′loxP) was cloned downstream of exon 5, and a PGKneo cassette flanked by FRT sites was cloned upstream of exon 2. The linearized targeting vector was introduced into C57BL/6J ESCs by electroporation, and cells were selected with G418. 96 G418-resistant ESC colonies were selected and screened for a recombination event using long-range PCR. The FRT-flanked Neo selection cassette was removed by subsequent FLPe-mediated recombination. Two ESC clones carrying one floxed *Pcgf6* allele were microinjected into C57BL/6J blastocysts to generate chimeric animals. Both ESC clones successfully transmitted the *Pcgf6*-flox conditional allele through the germline. These mice were mated with a mouse strain that expresses Cre recombinase ubiquitously under the control of the cytomegalovirus promoter. Deletion of exons 2–5 of the *Pcgf6* gene was confirmed by PCR analysis (Fig. 1*B*). Successful gene ablation of *Pcgf6* in homozygous *Pcgf6* ($Pcgf6^{-/-}$)-deficient mice was also confirmed by the absence of its protein product in multiple tissues by Western blotting analyses (Fig. 1*C*). Heterozygous *Pcgf6* mice were viable, fertile, and indistinguishable from WT littermates. When heterozygotes were intercrossed, we observed a significantly lower fraction of *Pcgf6* homozygous mutant offspring than the 25% predicted by the Mendelian law (Fig. 1*D*), which is consistent with previous results (12). Additionally, surviving homozygotes appeared smaller in body size and lighter in weight than their WT or heterozygous littermates at the same age (Fig. 1, *E* and *F*). Notably, ablation of *Pcgf6* did not affect the protein levels of other components of the PRC1.6 complex (Fig. 1*C*).

Mice deficient in Pcgf6 exhibit a strongly reduced fertility

qRT-PCR showed broad expression of *Pcgf6* mRNA in various tissues of WT mice, among which the highest level of expression was detected in testis (Figs. S1 and S2*A*). Moreover, recent research has demonstrated that ablation of the genes encoding the unique subunits of PRC1.6 in ESCs is accompanied with robust derepression of germline-specific gene expression (8, 10, 13, 17, 18). Thus, the unique expression patterns of *Pcgf6* prompted us to explore its potential regulation of reproduction and fertility in mice. When $Pcgf6^{+/-}$ males and females were crossed with their WT counterparts, the litter sizes (7.1 and 6.7 pups/litter, respectively) were slightly smaller than that after intercrossing the WT male and female mice (8.2 ± 1.2 pups) (Fig. 1*G*); however, crosses of $Pcgf6^{-/-}$ males and females with WT counterparts produced significantly smaller litters than did the controls (5.8 and 4.5 pups, respectively). It was noteworthy that mating of $Pcgf6^{-/-}$ mice produced an average litter size of only 1.7 pups (Fig. 1*G*). These data indicated that loss of *Pcgf6* in both male and female mice caused a reduction in fecundity.

To evaluate fertility in the male *Pcgf6* null mice, testicular development and morphology were analyzed. At 8 weeks postpartum, testes and epididymis from male $Pcgf6^{-/-}$ were smaller than those from WT littermates (Fig. 2*A*). When testes and epididymis weights were normalized to body weight, the ratios were significantly reduced in $Pcgf6^{-/-}$ mice compared with WT mice (Fig. 2*B*), suggesting an impairment of testicular function and/or spermatogenesis. Histological analysis of the testes by hematoxylin and eosin (H&E) staining indicated that there were no significant alterations in the interstitial spaces or seminiferous epithelium of testes from $Pcgf6^{-/-}$ mice (Fig. 2*C*). Meanwhile, as observed with the testis, H&E staining did not reveal any significant morphological differences in the ovaries of adult $Pcgf6^{-/-}$ mice compared with WT littermates (Fig. S2). However, compared with WT mice, $Pcgf6^{-/-}$ mice exhibited significant reductions in sperm motility, accompanied by more morphologically abnormal sperm than exhibited by WT littermates (Fig. 2, *D–F*). To gain insight into the molecular mechanisms underlying the observed phenotypic changes, we performed RNA-Seq on whole testes from $Pcgf6^{-/-}$ mice and their respective control. In $Pcgf6^{-/-}$ testes, 150 genes were deregulated (with 65 up-regulated and 85 down-regulated) on a -fold change cutoff of 2 and p value <0.05 (Fig. 2*G* and Table S3). Gene ontology (GO) analysis of down-regulated target genes scored them as being strongly related to sperm motility and differentiation (Fig. 2*H*), suggesting a particular role for Pcgf6 in sperm fate specification. In contrast, GO analysis of up-regulated genes did not show significant association with any biological process. Importantly, among down-regulated genes, our analysis revealed a set of genes, including *Adam7*, *Crisp1*, *Rnase9*, *Spinkl*, *Spink8*, *Spink10*, and *Ceacam10* (Fig. 2*I*), which have been shown to have critical roles in testicular development and function (19–25). Spermatogenesis and fertility depend upon functional interactions between germ cells and somatic cells (Leydig and Sertoli cells). To have a more in-depth understanding of Pcgf6 in spermatogenetic events, we isolated multiple testicular cell populations (Sertoli, Leydig, and several spermatogenic cell populations) from testes. Interestingly, although *Pcgf6* was expressed in Leydig and Sertoli cells, as well as in all types of germ cells of mouse testis, loss of the *Pcgf6* gene affected its target gene expression (such as *Crisp1*, *Rnase9*, and *Spinkl*) in germ cells at the round and elongating spermatid stage but not in somatic cells or pachytene spermatocytes, raising the possibility that Pcgf6 functions in a stage-dependent manner during spermatogenesis (Fig. S3).

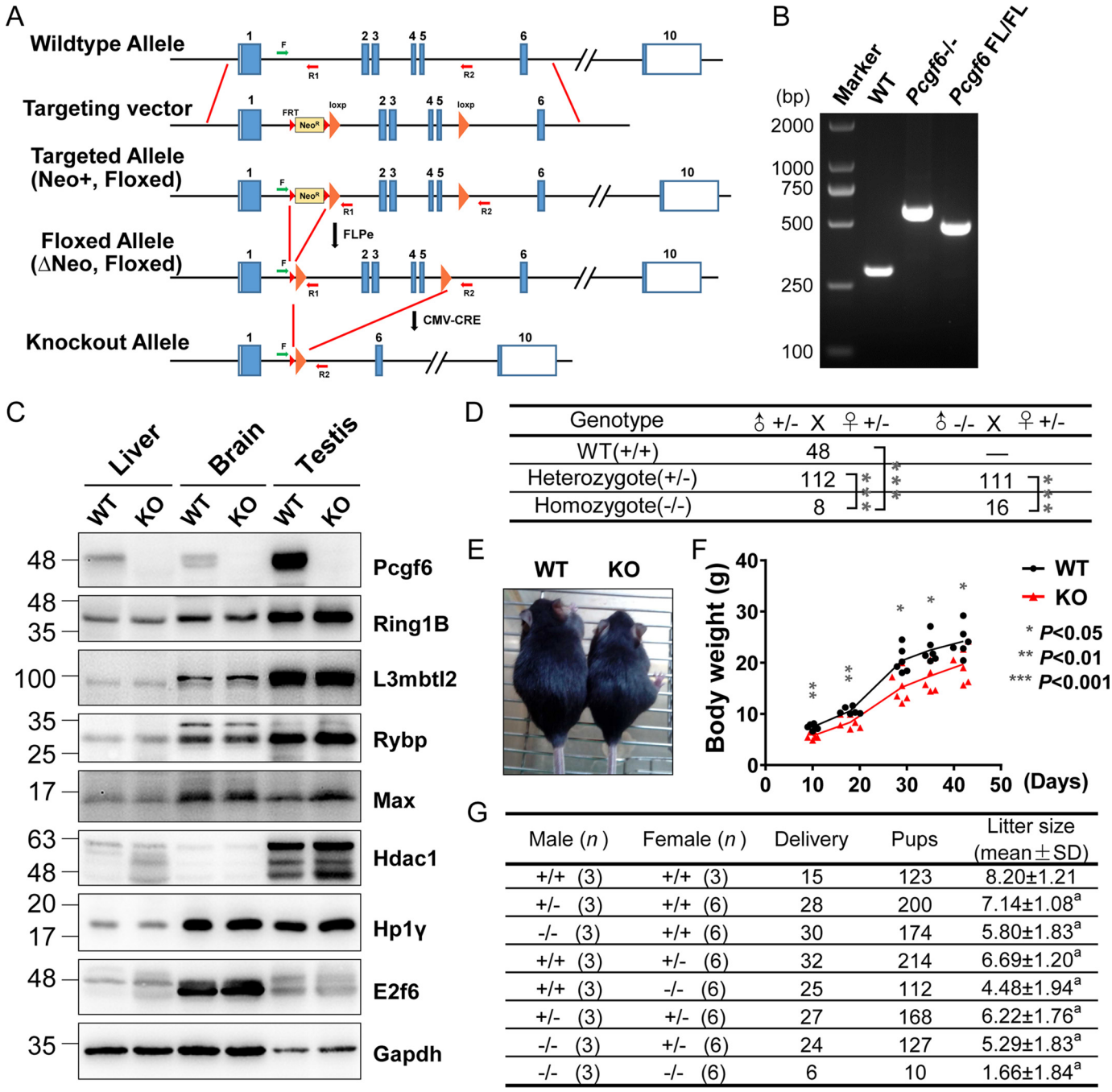

G

Male (*n*)	Female (*n*)	Delivery	Pups	Litter size (mean±SD)
+/+ (3)	+/+ (3)	15	123	8.20±1.21
+/- (3)	+/+ (6)	28	200	7.14±1.08[a]
-/- (3)	+/+ (6)	30	174	5.80±1.83[a]
+/+ (3)	+/- (6)	32	214	6.69±1.20[a]
+/+ (3)	-/- (6)	25	112	4.48±1.94[a]
+/- (3)	+/- (6)	27	168	6.22±1.76[a]
-/- (3)	+/- (6)	24	127	5.29±1.83[a]
-/- (3)	-/- (6)	6	10	1.66±1.84[a]

Figure 1. *Pcgf6* null mice exhibit partially penetrant embryonic lethality. *A*, schematic of the gene targeting strategy used to generate *Pcgf6* mutant mice. The WT *Pcgf6* locus is shown at the *top*. The targeting vector contains loxP sites flanking exons 2–5 and a neomycin gene flanked by FRT sites. F, R1, R2 are primers used to determine genotypes. *B*, genomic PCR for analysis of *Pcgf6* gene status. The primers F, R1, and R2 shown in *A* and DNA from toes of mice were used to determine genotypes. *C*, Western blotting demonstrating changes in the protein levels of the indicated genes in the liver, brain, and testis of indicated genotypes. Protein loading is 40 μg. Gapdh was used as a control. *D*, genotype distribution of progeny of different intercrosses. ***, $p < 0.005$ (χ^2 test), indicating that the probability of conforming to the Mendelian law is <0.5%. *E*, body size of the $Pcgf6^{+/+}$ and $Pcgf6^{-/-}$ mice at 6 weeks. *F*, body weight of $Pcgf6^{-/-}$ mice from birth to adulthood compared with WT mice. $n = 6$. *G*, fecundity of $Pcgf6^{+/+}$, $Pcgf6^{+/-}$, and $Pcgf6^{-/-}$ mice. *n*, number of mice. *a*, $p < 0.01$(*t* test) *versus* +/+ × +/+.

Together, our studies suggest a previously unknown role for Pcgf6 in testicular development and spermatogenesis.

Germline-specific genes are aberrantly expressed in Pcgf6 null adult somatic tissues

Given that genetic ablation of *Pcgf6* in ESCs results in illegitimate expression of germ cell– and meiosis–related genes, we wondered whether Pcgf6 is functionally required for the silencing of germline genes in somatic tissues (10, 12). To this end, we compared the expression profiles of liver and brain (organs that show the high *Pcgf6* mRNA expression levels (Fig. S1)) from *Pcgf6* knockout and littermate WT control mice by RNA-Seq analysis. A total of 160 *versus* 61 genes were considerably up-regulated in *Pcgf6*-deficient liver and brain, respectively, and 50 *versus* 56 down-regulated genes in *Pcgf6*-deficient liver

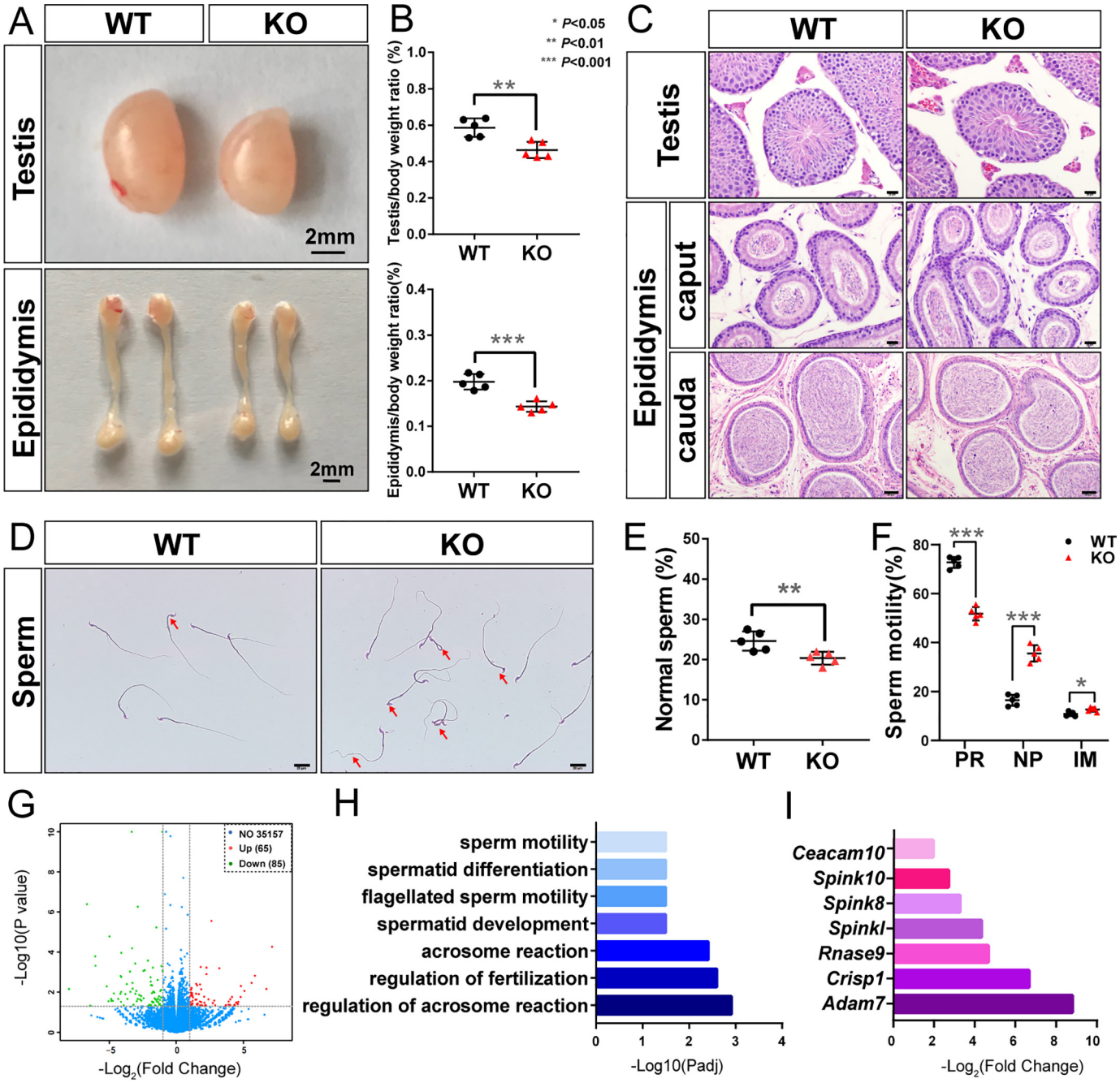

Figure 2. *Pcgf6*-deficient mice dramatically reduced in fertility. *A*, representative image of the testes and epididymides of the WT and *Pcgf6*$^{-/-}$ mice. *Scale bars*, 2 mm. *B*, testis and epididymis as a percentage of body weight of mice with the indicated genotype. *C*, H&E staining of representative sections of the testes and epididymis of the WT and *Pcgf6*$^{-/-}$ mice. *Scale bars*, 50 μm (cauda epididymis) or 20 μm (others). *D*, normal and abnormal sperms in WT and *Pcgf6*$^{-/-}$ mice at 8 weeks of age. *Red arrows*, defective sperms. *E* and *F*, the proportions of normal sperm and the sperm motility of mice with the indicated genotype at 8 weeks of age. Data are represented as the means ± S.D. (*error bars*) from five mice for each genotype. Sperm motility was measured using a CASA CEROS version 12 sperm analysis system (Hamilton Thorne). *PR*, progressively motile; *NP*, nonprogressively motile; *IM*, immotile. *G*, volcano plot of differentially expressed genes in testis between WT and *Pcgf6*$^{-/-}$ mice. *H*, GO analyses showing the biological functions of down-regulated genes in *Pcgf6*$^{-/-}$ testis. *I*, the $\log_2$(-fold change) of the several down-regulated genes related to sperm function in *Pcgf6*$^{-/-}$ testis.

and brain, respectively, compared with their corresponding controls (Fig. 3 (*A* and *C*) and Tables S4 and S5). To gain insight into the physiological functions of Pcgf6-mediated gene regulation in somatic tissues, we performed gene ontology (GO) analyses, which revealed that the up-regulated genes are significantly enriched in germ cell– and meiosis–related functions (Fig. 3*B*). Strikingly, analysis of genes commonly up-regulated in *Pcgf6*-deficient liver and brain revealed highly significant overlap between the two RNA-Seq datasets, and GO analysis of these overlapping genes again demonstrated a strong enrichment of terms involved in meiosis and germ cell development (Fig. 3, *C* and *D*). By contrast, no significant association to any pathways or biological processes was identified in the down-regulated gene group. Together, these data revealed a previously unappreciated function of Pcgf6 for suppressing genes associated with germ cells and meiosis in cell types other than

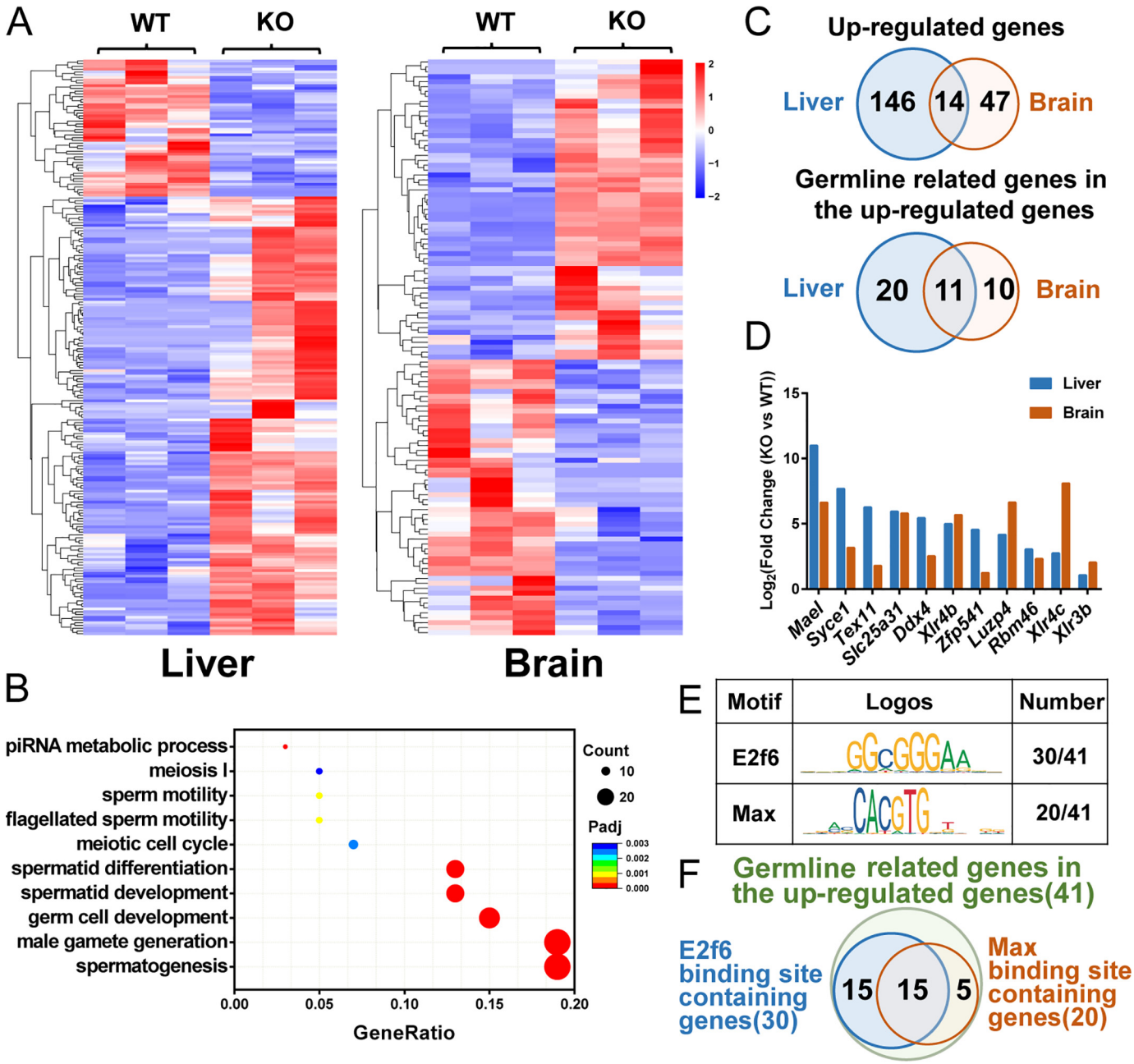

Figure 3. Pcgf6 represses the expression of germline-related genes with binding sites of Max and E2f6 in the liver and brain. *A*, RNA-Seq heat map of transcripts with 2-fold expression differences and $p < 0.05$ in liver and brain comparing WT mice with *Pcgf6*$^{-/-}$ mice. *B*, GO analysis of biological functions of 207 up-regulated genes in the liver and brain. *C*, Venn diagrams of up-regulated target genes and germline-related genes in the liver and brain of *Pcgf6*$^{-/-}$ mice. *D*, $\log_2$(-fold changes (KO *versus* WT)) in the expression of the 11 germline-related genes up-regulated in both liver and brain. *E*, motif analysis of 41 germline-related genes in up-regulated genes of liver and brain. *F*, the overlap between E2f6-binding sites containing genes and Max-binding sites containing genes.

ESCs. Interestingly, we examined the proximal promoter regions of 41 up-regulated germ cell–specific genes and found specific enrichment of the binding motifs for E2f6/Dp1 (GCGGGAA) (26) and Mga/Max (the E-box, CACGTG) (27) (Fig. 3, *E* and *F*). The presence of centrally enriched E-box and E2f6/Dp1 motifs in these germ cell promoters suggests that Pcgf6 represses germ cell gene expression in the context of a PRC1.6 complex.

To build on this observation, we next chose to focus our efforts on the set of germline-specific genes showing aberrant expression in adult somatic tissues derived from *Pcgf6* null mice. qRT-PCR analysis of *Ddx4*, *Luzp4*, *Mael*, *Syce1*, *Slc25a31*, *Rbm46*, *Tex11*, and *Xlr4c* mRNA confirmed that expression of these genes was undetectable in WT somatic tissues, whereas they were derepressed in liver and brain but also in all of the tissues we tested derived from *Pcgf6* null adult mice (Fig. 4). From these results, we concluded that Pcgf6 is primarily involved in suppression of the germ cell lineage differentiation program in somatic cells and tissues.

Because *Pcgf6* is highly expressed in ESCs and contributes to the repression of germline genes in somatic cells, we postulated that Pcgf6 may be required for somatic cell reprogramming. To explore this possibility, we reprogrammed mouse embryonic

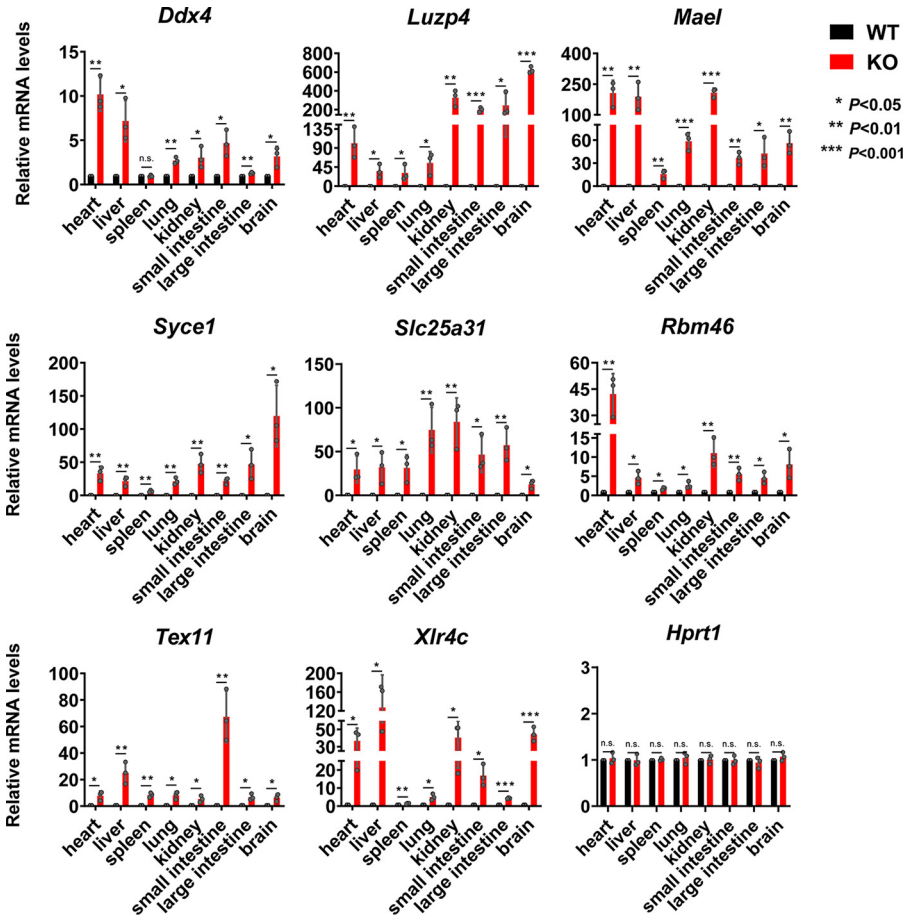

Figure 4. Pcgf6 represses the expression of germline-related genes almost in all somatic organs. Relative expression of the indicated germline-related genes in various tissues of *Pcgf6*$^{-/-}$ mice determined by qRT-PCR. *Actin* was used as a control for normalization. *Hprt1* was used as a negative control. Data are from three biological replicates each with three technical replicates. *Error bars*, S.D. *n.s.*, nonsignificant (two-tailed Student's *t* test).

fibroblasts (MEFs) derived from the *Pcgf6*$^{-/-}$ mice using the classical Yamanaka's method (28). As shown in Fig. S4, *Pcgf6* deficiency in MEFs dramatically reduced the formation of alkaline phosphatase–positive colonies in Oct4-, Sox2-, Klf4-, and c-Myc (OSKM)-driven reprogramming. Importantly, reprogramming efficiency of *Pcgf6*$^{-/-}$ MEFs could be rescued by transduction of *Pcgf6* (Fig. S4). The requirement for Pcgf6 in somatic cell reprogramming was also reported in recent studies using an shRNA-mediated knockdown approach (11). Taken together, these studies reveal that Pcgf6 is specifically implicated in somatic cell reprogramming.

DNA methylation is largely dispensable for Pcgf6-mediated germline gene silencing

Promoter CpG island DNA methylation is generally associated with gene silencing (29). A cluster of X-linked germ line–specific genes has been reported to be derepressed in cells deficient in DNA methyltransferases (30). Therefore, we asked whether the up-regulation of germ cell–specific genes in *Pcgf6* null cells would be accompanied by changes in promoter DNA methylation. The content in methylated cytosines in the proximal promoters of the four selected genes, which were significantly up-regulated in *Pcgf6* null somatic tissues (Fig. 4), was determined by conventional Sanger sequencing bisulfite-assisted genomic DNA. As shown in Fig. S5, following *Pcgf6* inactivation, the promoter-proximal CpG islands of *Ddx4*, *Mael*, and *Slc25a31* underwent marginal DNA demethylation, whereas *Syce1* showed no differences from WT liver. By contrast, *Pcgf6* deficiency in testis had no detectable effect on DNA methylation in the proximal CpG islands of these four genes, consistent with the unaltered mRNA levels in testis after deletion of *Pcgf6* (Fig. S5). Together, these results suggest that maintenance of DNA methylation patterns is not essential for Pcgf6-mediated repression of germ cell–specific gene expression.

Pcgf6 associates with G9a/glp and Hdac1/2 and directs them to its target promoters to repress germ cell–related genes

Generally, repressors recruit multiple cofactors involved in histone deacetylation and methylation or chromatin remodeling to mediate concerted transcriptional silencing via multiple repression pathways (29). Interestingly, Hdac1/2 and G9a/Glp have repeatedly been identified as additional subunits of PRC1.6 (6, 8,9, 12). The presence of Hdac1/2 and G9a/Glp in Pcgf6-PRC1 complex prompted us to assess whether these epigenetic regulators associate with Pcgf6 to cooperatively repress germ cell–related genes. We explored this possibility via biochemical and genetic analyses. First, we examined interactions between Pcgf6 and these four epigenetic regulators in mouse

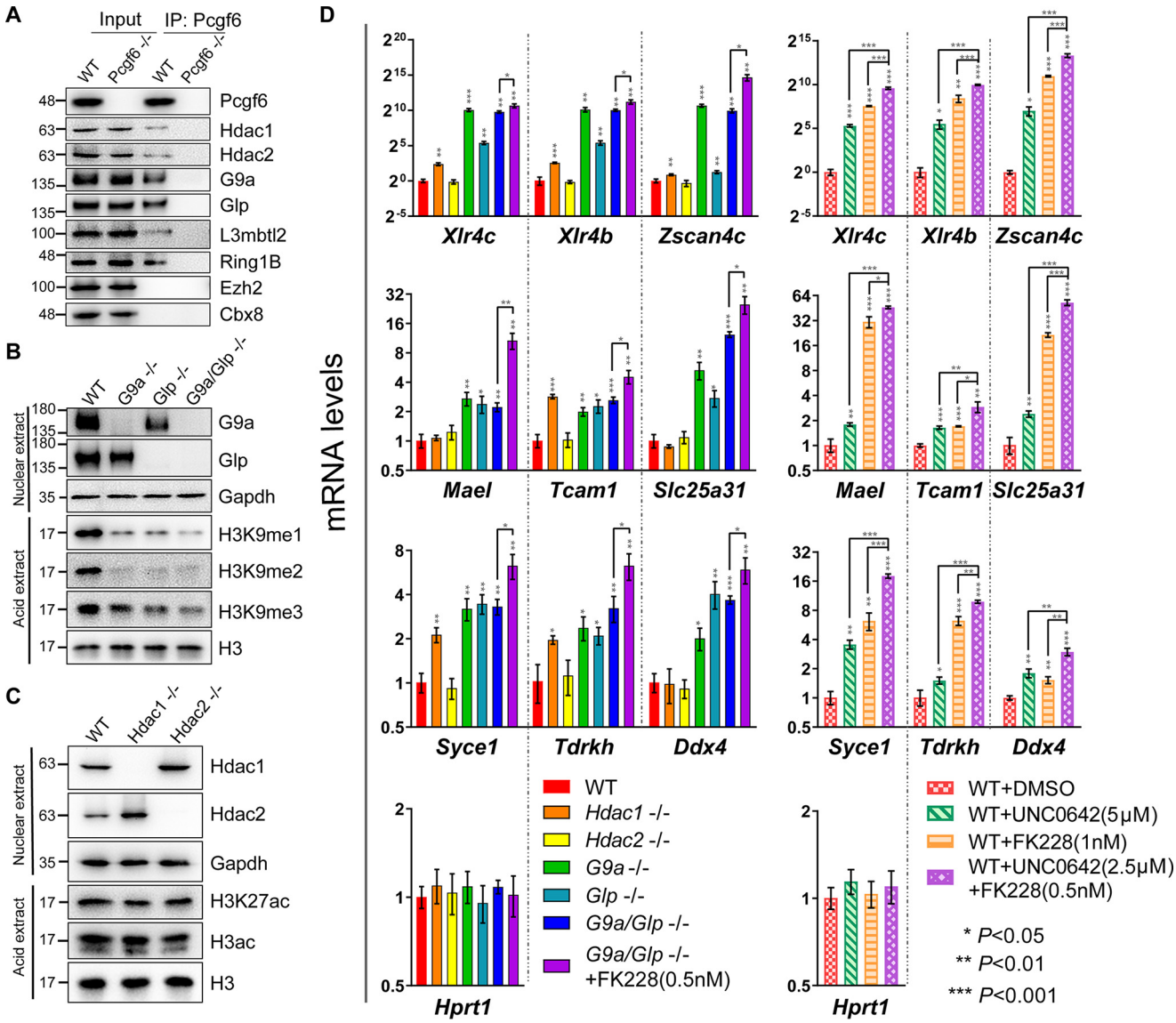

Figure 5. G9a/Glp and Hdac1/2 repress the expression of Pcgf6 targeted germline genes. *A*, IP–Western blot analysis showing physical interaction of Pcgf6, Hdac1/2, and G9a/Glp in cell extracts from WT and *Pcgf6*$^{-/-}$ ESCs. *B*, Western blot analysis showing the methylation levels of H3K9 in *G9a*$^{-/-}$, *Glp*$^{-/-}$, and *G9a/Glp*$^{-/-}$ ESCs. *C*, Western blot analysis showing the acetylation levels of H3 in *Hdac1*$^{-/-}$ and *Hdac2*$^{-/-}$ ESCs. *D*, the mRNA levels of germline-related genes in ESCs of the indicated genotype or in ESCs treated with the indicated inhibitors. All cells were treated with inhibitors for 72 h. DMSO is the solvent control. *Error bars*, S.D. of three independent experiments. The *asterisks arranged vertically* refer to significant differences compared with WT ESCs. *Horizontally arranged asterisks* indicate significant differences between groups.

ESCs by co-immunoprecipitation assays. As shown in Fig. 5*A*, both the Hdac1/2 and the G9a/Glp as well as L3mbtl2 and Ring1B proteins were co-immunoprecipitated with anti-Pcgf6 antibody, whereas deletion of Pcgf6 resulted in undetectable G9a/Glp or Hdac1/2 in the precipitates. In contrast, the interaction of Pcgf6 with Ezh2 and Cbx8, a histone H3K27 methyltransferase and a canonical PRC1 subunit, respectively, was not detected, indicating that interaction between Pcgf6 and the individual G9a/Glp and Hdac1/2 is specific. To further explore whether Pcgf6 could interact directly with G9a/Glp and Hdac1/2, we purified recombinant GSH *S*-transferase (GST)-tagged Pcgf6, His-Ring1B, His-G9a/Glp, and His-Hdac1/2 and measured their direct interactions using a GST pulldown assay. We found that Pcgf6 selectively recognized Ring1B and did not exhibit detectable binding to G9a/Glp or Hdac1/2, likely suggesting that Pcgf6 interacts with G9a/Glp and Hdac1/2 through other PRC1.6 subunits (Fig. S6).

Second, to test the requirement of these histone-modifying enzymes for repression of germ cell–related genes, we generated single or double knockout of *Hdac1/2* and *G9a/Glp* ESCs using CRISPR/Cas9 technology (31–33) (Figs. S7 and S8). The successful knockout of these enzymes was confirmed by genomic PCR and Western blotting (Fig. 5 (*B* and C) and Figs. S7 and S8). Consistent with previous reports, *G9a* or *Glp* single deficient ESCs lacked nearly all of the H3K9me2 and showed a significant decrease in H3K9me1, whereas H3K9me3 levels were mildly affected (Fig. 5*B*). Interestingly, double knockout of *G9a/Glp* further reduced the methylation level of H3K9me3 but not H3K9me1 or H3K9me2, suggesting that G9a and Glp generally cannot compensate for the function of each other (34,

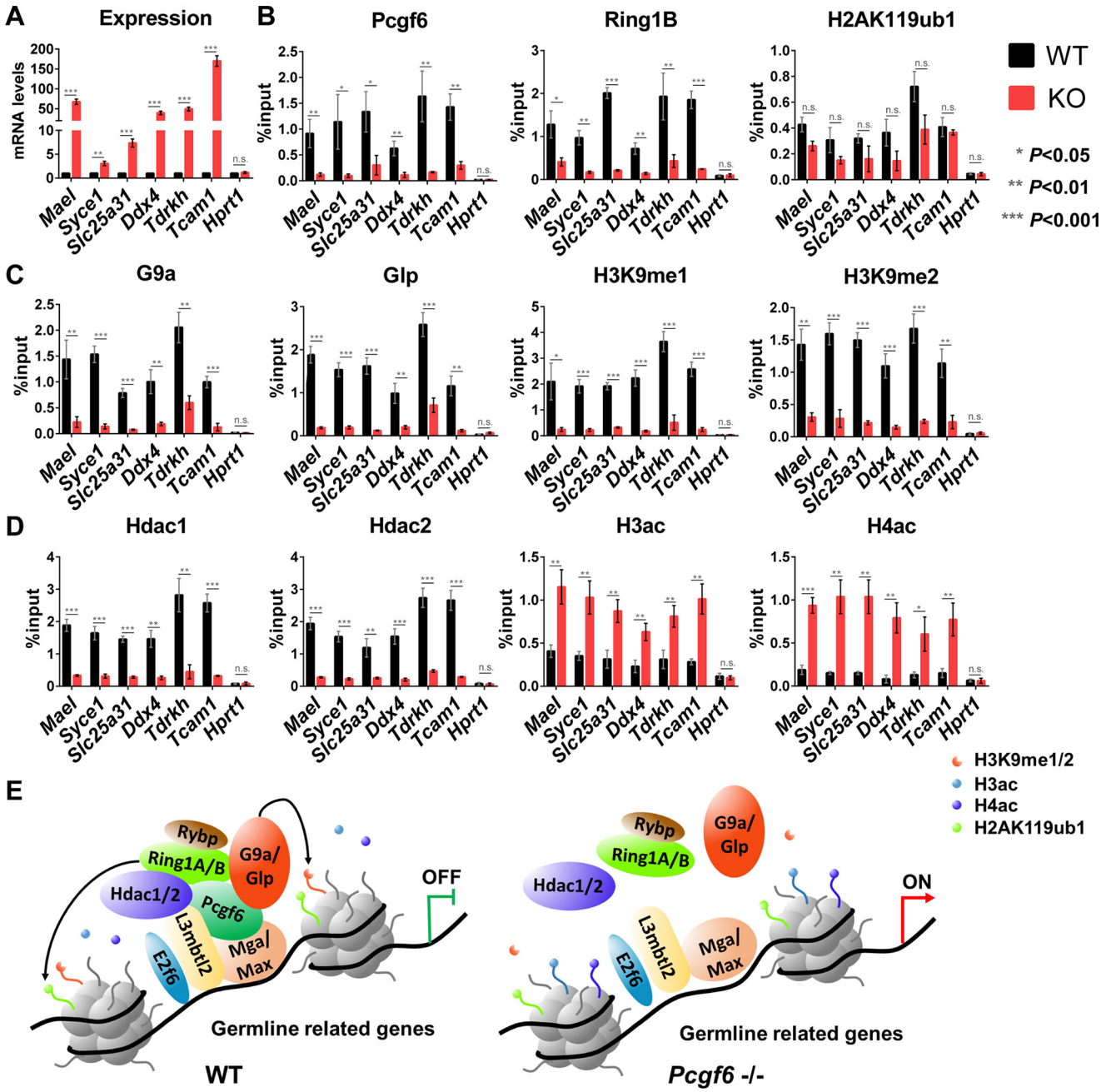

Figure 6. Pcgf6 plays a key role in recruiting G9a/Glp and Hdac1/2 to germline-related genes. *A*, mRNA expression analysis of the selected genes in ESCs of the indicated genotype. *B–D*, ChIP-qPCR analysis showing enrichment of the indicated proteins on the selected gene promoters in WT and *Pcgf6*$^{-/-}$ ESCs. *Error bars*, S.D. of three independent repeats. *E*, a schematic model showing that recruiting Hdac1/2 and G9a/Glp is an important mechanism used by Pcgf6 to modify histone tails and repress the expression of germline-related genes (see "Discussion" for a detailed description).

35). As reported previously (36), individual *Hdac1/2* disruption in ESCs was not associated with changes in chromatin modifications altered by these enzymes (*i.e.* histone 3 acetylation (H3ac) and H3K27ac) (Fig. 5*C*). As expected, the expression of the germline genes, including *Xlr4c*, *Xlr4b*, *Zscan4c*, *Mael*, *Tcam1*, *Slc25a31*, *Syce1*, *Tdrkh*, and *Ddx4*, in ESCs with single deficiency of *G9a*/*Glp* was significantly up-regulated, as evidenced by qRT-PCR. Comparing expression changes of germ cell–related genes in single mutant cells with those in cells with combined inactivation of *G9a/Glp*, we observed no synergistic effects (Fig. 5*D*). In agreement with these results, the G9a/Glp inhibitor UNC0642-treated WT ESCs displayed a significant induction of germ cell–related gene expression. Interestingly, despite the fact that *Hdac1*, but not *Hdac2*, single knockout displayed a mild effect on derepression of germ cell–related genes, Hdac1/2-selective inhibitor FK228 significantly induced the expression of these genes, suggesting functional redundancy between these two Hdacs (Fig. 5*D*). In addition, Hdac1/2 inhibitor treatment of *G9a*/*Glp* double null ESCs further enhanced the expression of germline genes. Likewise, FK228 in combination with UNC0642 in ESCs showed strong synergistic effects (Fig. 5*D*). Together, these data suggest a possible synergistic cooperation between the two enzymatic activities.

The above results establish a role for G9a/Glp and Hdac1/2 in the repression of germ cell–related genes; however, the molecular mechanism by which they are targeted to a small subset of promoters is not understood. Given that Pcgf6 interacts with G9a/Glp and Hdac1/2, we wondered whether it is directly involved in recruitment of these proteins. We first examined the association between Pcgf6 and the promoters of known target genes (10) (Fig. 6*A*) via ChIP assays by anti-Pcgf6 antibodies (Fig. 6*B*). We found that the Pcgf6 was enriched at the promoters of selected germ cell–related genes—including *Mael*, *Tcam1*, *Slc25a31*, *Syce1*, *Tdrkh*, and *Ddx4*—whereas enrichment of Pcgf6 was not observed at the promoter of *Hprt1*, whose expression in ESCs was not changed by absence of *Pcgf6* (Fig. 6*B*). Importantly, this was accompanied by considerable enrichment of Ring1B, G9a/Glp, and Hdac1/2, suggesting that Pcgf6 is involved in the recruitment of the PRC1.6 complex (Fig. 6, *B–D*). Accordingly, we observed association of H3K9me1 and H3K9me2 with the indicated target genes. Moreover, enrichment of Ring1B, G9a/Glp, Hdac1/2, H3K9me1, and H3K9me2 (but not H3K9me3) at the target promoters was indeed markedly depleted in the absence of *Pcgf6* (Fig. 6 (*B–D*) and Fig. S9), whereas their global levels remained largely unperturbed following loss of *Pcgf6* (Fig. 5*A* and Fig. S10). ChIP analysis of histone 3 and histone 4 acetylation (H3ac and H4ac) revealed that histone acetylation at Pcgf6-bound promoters increased dramatically after disruption of *Pcgf6* (Fig. 6*D*), consistent with reduced local activity of Hdac1/2 (Fig. 6*D*). Notably, consistent with our previous report (10, 37), H2AK119ub1 enrichment at these targets did not show considerable changes in the *Pcgf6* null ESCs despite substantially depleted Ring1B occupancy (Fig. 6*B*). This finding agrees with the observation that Pcgf1-PRC1 complex is essential for shaping normal H2AK119ub1 and Pcgf6-PRC1 complex is a weak ubiquitin ligase in ESCs *in vivo* (38). Together, these results suggest that Pcgf6 coordinates epigenetic repression of germ cell–related genes by recruitment of G9a/Glp and Hdac1/2 (Fig. 6*E*).

Discussion

We reported here that targeted disruption of polycomb protein Pcgf6 in mice resulted in partially penetrant embryonic lethality, and surviving mutants displayed markedly impaired fertility. Taking advantage of *Pcgf6*-deficient mice, we showed that Pcgf6 targets were enriched for meiosis– and germ cell–related genes in liver and brain and that such genes were dramatically derepressed in all *Pcgf6* null tissues we examined. Mechanically, Pcgf6 recruited G9a/Glp and Hdac1/2 to modify the promoter region of these germline genes targeted for repression by Pcgf6. Our work thus shows a link between target promoters tethering by Pcgf6 with transcriptional silencing of germ cell–specific genes by G9a/Glp and Hdac1/2.

Histone H3K9 methylation is generally linked to gene repression, and G9a/Glp is reported to be targeted to selected gene promoters by sequence-specific DNA-binding factors (7). Additionally, G9a has been shown to associate with transcription factors CDP/cut, PRDI-BF1, Gfi1, and SHP and is recruited to their correspondingly targeted sites (39–42). Importantly, each of these G9a-interacting transcription factors also associates with Hdacs. Here, we have shown that Pcgf6 targets the action of both G9a/Glp and Hdac1/2 to the promoters of germline genes to dictate the transcriptional silencing of germline genes in ESCs, even though the precise molecular mechanisms by which it exerts this function still need further investigation. Of note, we recently reported that efficient recruitment of PRC1.6 depends on functional cooperation among unique subunits (L3mbtl2, Max, Mga, and Pcgf6) in the complex (37). Consistently, knockout of the genes encoding these unique subunits of PRC1.6 is accompanied with induction of germline gene expression (8, 10, 12, 17, 18). Intriguingly, deletion of *Max* in ESCs results in marked cytological changes reminiscent of meiotic cell division (17, 43). Therefore, *Pcgf6* ablation–mediated selective derepression of germline genes reflects the impairment of PRC1.6 in which Pcgf6 is one of the important components. In further support of this scenario, our analysis of the proximal promoters of derepressed germline genes following genetic ablation of the *Pcgf6* gene allowed the identification of putative signature motifs for Pcgf6 target genes, with the general enrichment of the E2f6/Dp1- and Mga/Max-binding sites (26, 27). It is worth mentioning that Ring1B, which is a major common subunit of PRC1, has been reported to be required for repression of *Stra8* and other germline genes driving meiosis (44). This strongly indicates the existence of additional machineries for germline gene repression. Of particular interest, at selected Pcgf6 target promoters, Ring1B occupancy coincides with low or undetectable H2AK119ub1 levels, and the H2AK119ub1 signals were not compromised by loss of Pcgf6, suggesting that Pcgf6 complex could play a role at these promoters that is largely independent from its ability to modify histone H2A. It has been reported, however, that in ESCs from the conditional targeting, H2AK119ub1 occupancy is reduced in the absence of *Pcgf6*, implying the contribution of H2AK119ub1 in Pcgf6-mediated gene repression (12). This discrepancy might arise from differences in gene targeting approaches (conditional *versus* constitutive) used. Notably, our observation is in line with a recent report demonstrating a pivotal role of Pcgf1-PRC1 in shaping normal H2AK119ub1 in ESCs (38). Further studies are needed to explore the potential link between H2AK119ub1 and Pcgf6-mediated gene silencing. On the basis of these findings, we propose that Pcgf6 forms a complex with Hdac1/2 and G9a/Glp in undifferentiated ESCs as well as specified cell types and represses the expression of germline genes via repressive histone modification, namely histone deacetylation and H3K9 methylation (Fig. 6*E*).

PcG proteins are traditionally described as transcriptional repressors (1, 3). However, they can also bind to active promoters, where they mediate positive regulation of gene expression (45–47). A substantial number of expression changes with germ genes being down-regulated in *Pcgf6* null testes may imply an additional role for Pcgf6 in germline-specific gene regulation. Pcgf6 may in fact play dual roles as both an activator and a repressor. Its functions may be determined by cell/tissue type and by differences in the complexes with which Pcgf6 is associated. For instance, in somatic tissues and ESCs, Pcgf6 represses transcription by acting as a platform upon which multiple factors that mediate gene silencing are assembled. Most notably, these include transcriptional repressors Hdac1/2

and G9a/Glp, thereby contributing to silencing of active chromatin. In meiotic cells, Pcgf6 may instead be recruiting an activation complex to meiosis-specific genes. We hypothesize that deregulated expression of these germline genes upon *Pcgf6* ablation contributes to the observed phenotypes in spermatogenesis. Indeed, *Pcgf6* and *L3mbtl2* knockout mice exhibited a severely impaired spermatogenesis (Fig. 2) (48), supporting this notion. The function of Pcgf6 for key steps of spermatogenesis needs to be further elucidated. Given that the functionality of the PRC depends on its diverse biochemical composition, Pcgf6-containing PRC1 may consist of two or more subsets of complexes, thus allowing it to act as both an activator and a repressor. Further proteomic investigation of Pcgf6 protein interactome is required to gain deeper insights into the diverse functions of Pcgf6 in ESCs and multiple types of specialized cells.

Experimental procedures

Generation of Pcgf6$^{-/-}$ mice

Pcgf6-targeting vectors containing loxP sites flanking exons 2–5 and a Neo flanked with FRT sites were linearized and then introduced into C57BL/6 ESCs and selected by G418. The Neo cassette was deleted by transfecting a vector expressing FLPe recombinase. Chimeras were generated by injecting correctly targeted ESCs into C57BL/6J blastocysts. The consequent male chimeric mice were bred with female C57BL/6 mice, and germ line transmission of the *Pcgf6*-targeted (*Pcgf6*$^{FL/+}$) allele was examined in the offspring. Conditional single allele mice were mated with cytomegalovirus-Cre transgenic mice to generate heterozygous mice for the *Pcgf6* deficiency. The homozygous knockout mice (KO, *Pcgf6*$^{-/-}$) were produced by intercrossing of *Pcgf6*$^{+/-}$ male and female mice. Genotyping primers are given in Table S1. The experimental animal facility has been accredited by the Association for Assessment and Accreditation of Laboratory Animal Care International, and the institutional animal care and use committee of the Model Animal Research Center of Nanjing University approved all animal protocols used in this study.

Generation of mutant cell lines and cell culture

Construction and transfection of Cas9 vector with a single guide RNA (sgRNA) were performed as described previously (10). Briefly, sgRNAs of the genes of interest were designed by the CRISPR design tool (RRID:SCR_015935) (33) and cloned into PX459 vector. pSpCas9(BB)-2A-Puro (PX459) V2.0 was a gift from Feng Zhang (Addgene plasmid 62988; RRID:Addgene_62988). After a 24-h transfection with the plasmids expressing a pair of sgRNAs and a puromycin resistance plasmid by Lipofectamine 2000 (Thermo Fisher Scientific), mouse ESCs were selected by puromycin for 2 days and then seeded on mitomycin-irradiated feeder cells in ESC medium. The null ESC clones were identified by genomic PCR analysis, qRT-PCR, and Western blotting. As previously described, ESCs were cultured in Dulbecco's modified Eagle's medium high glucose (Gibco) with 15% fetal calf serum (Gibco), L-glutamine (Gibco), nonessential amino acids (Gibco), β-mercaptoethanol (Sigma), 1000 units/ml leukemia inhibitory factor, and penicillin/streptomycin (Gibco).

Histology and immunohistochemistry

Tissues were harvested and fixed with 4% paraformaldehyde overnight at 4 °C and then dehydrated and embedded in paraffin. 5-μm-thick paraffin sections were stained with H&E or used for immunohistochemistry. Images were obtained by BX53 semi-electric fluorescence microscope (Olympus).

Fertility and fecundity assessment

Fertility and fecundity assessment was performed as described previously (49, 50). Briefly, *Pcgf6*$^{+/-}$ and *Pcgf6*$^{-/-}$ littermate males (>8 weeks old) were placed with WT fertile females of 2–6 months of age, respectively. *Pcgf6*$^{+/-}$ and *Pcgf6*$^{-/-}$ littermate females were caged with mature WT males for a similar period. The presence of a copulatory plug among females was checked over the first 4 days. Females with copulatory plug were either left with the male or removed to another cage and then checked again at 3 weeks for pregnancy. The number of offspring from each pregnancy was recorded.

Sperm collection, motility and morphology test

To assess the effect of *Pcgf6* deficiency on sperms, the left and right caudal epididymitis of sexually mature mice were dissected out, minced in prewarmed TYH medium at 37 °C, and incubated for 120 min. The sperm suspension was filtered through a 70-μm nylon cell strainer to remove tissue debris. Sperm motility was then measured using a CASA CEROS version 12 sperm analysis system (Hamilton Thorne). The analysis setting described previously was used (51). To evaluate sperm abnormalities in *Pcgf6*-deficient mice, we made a thin smear of sperm air-dried on a premarked cleaned glass slide. After staining with a Diff-Quik stain kit (Solarbio, G2572) according to the instructions, 200 spermatozoa were examined per mouse using bright field illumination at ×400 magnification for normal and abnormal. All slides were coded for avoiding scorer biasness. Sperm normality was expressed as a percentage.

Transcriptome sequencing and analysis

For RNA-Seq, total RNA was extracted from the indicated tissues of WT and *Pcgf6*$^{-/-}$ mice, respectively, by the TRIzol reagent (Thermo Fisher Scientific) according to the manufacturer's instructions and sequenced by Novogene (Beijing, China). Briefly, sequencing libraries were constructed using the NEBNext® Ultra™ RNA Library Prep Kit for Illumina® (New England Biolabs) and assessed on the Agilent Bioanalyzer 2100 system. The library preparations were sequenced on an Illumina Hiseq platform. For data analysis, genes with a p value of <0.05 and 2-fold expression differences found by DESeq2 were considered as differentially expressed. GO enrichment analysis of differentially expressed genes was accomplished by the cluster Profiler R package. GO terms with corrected p value <0.05 were considered significantly enriched by differential expressed genes. We performed motif-scanning analysis using the online tool FIMO (RRID:SCR_001783). RNA-Seq data were available

from the Gene Expression Omnibus under accession number GSE143206.

Quantitative RT-PCR

The indicated tissues of mice and ESCs were harvested and lysed in TRIzol reagent (Thermo Fisher Scientific). Total RNA was extracted as described previously (10). Gene expression was quantified in triplicates on a Roche Light Cycler using PowerUp™ SYBR Green Master Mix (Thermo Fisher Scientific) with the primers shown in Table S1. Relative changes in transcript levels were analyzed using the $2^{-\Delta\Delta Ct}$ method. Values were normalized to *β-actin* mRNA content.

Conventional bisulfite sequencing

Genomic DNA was extracted from the liver and testis of WT and *Pcgf6*$^{-/-}$ mice using a Qiagen DNeasy blood and tissue kit and bisulfite-converted using the Qiagen Epitect bisulfite kit according to the provided instructions. The forward and reverse primers for the forward strand were designed by the online primer design tool Methprimer (RRID:SCR_010269), shown in Table S1 (52). The targeted regions were PCR-amplified from bisulfite-converted DNAs using Phanta Max Super-Fidelity DNA Polymerase (Vazyme, P505). The purified PCR products were subsequently cloned into pBluescript II KS(−) vectors using ClonExpress II (Vazyme). To reveal the methylation status of individual CpG sites in the promoter of the selected genes, we sequenced 20 single clones using conventional Sanger sequencing.

Whole-cell lysates, histone extraction, and Western blotting

Whole-cell lysates and histone extraction were performed as described previously (10). Briefly, ESCs were washed with ice-cold PBS containing 5 mM sodium butyrate twice, lysed with a Triton extraction buffer (PBS, 0.5% Triton, 2 mM phenylmethylsulfonyl fluoride, 0.02% NaN_3), and centrifuged. The pellet was resuspended in 0.2 N HCl after removing the supernatant. The histone was extracted overnight at 4 °C, and the supernatant was saved after centrifuging for 10 min Proteins were separated via SDS-PAGE and analyzed by immunoblotting. The antibodies used in this study are shown in Table S2.

GST pulldown assay

Expression and purification of GST or His tag fusion proteins were done as described previously (37). The GST pulldown assay was performed using the Pierce™ GST Protein Interaction Pull-Down Kit (Thermo Fisher Scientific, catalog no. 21516) according to the manufacturer's protocol. Aliquots of 50 μl of beads immobilized with GST or GST-Pcgf6 fusion proteins were incubated in 1 ml of binding buffer for 3 h at 4 °C. Then the GST-bound beads were washed three times with binding buffer. The His tag fusion protein was added to the beads, and after 3 h of gentle rocking motion on a rotating platform at 4 °C, the tube was centrifuged and washed three times with the wash buffer. The bait- and prey-bound proteins were separated by SDS-PAGE and detected by Western blotting with the indicated antibodies.

MEF isolation and iPS reprogramming

To analyze the effects on *Pcgf6* deficiency for iPS reprogramming, MEF isolation and iPS reprogramming were performed as described previously (28). Briefly, MEFs were isolated from embryonic day 13.5 WT and *Pcgf6*$^{-/-}$ embryos, respectively, and cultured in MEF medium (Dulbecco's modified Eagle's medium supplemented with 10% fetal calf serum, 2 mM L-glutamine, 100 units/ml penicillin/streptomycin, and 1 mM sodium pyruvate). MEFs were reprogrammed to iPS cells by lentiviral transduction. Lentivirus encoding Oct4, Sox2, Klf4, or c-Myc were generated by transfecting 293T cells as described previously (8). Viral supernatants from different transfections were equally mixed. WT and *Pcgf6*$^{-/-}$ MEFs were incubated with virus mixtures in the presence of Polybrene (Sigma; 8 μg/ml) for 24 h, and then supernatant was exchanged for MEF medium. 24 h later, infected cells were seeded onto mitomycin-irradiated WT MEFs and cultured in ESC medium. 3 weeks after transduction, the cells were stained using the Alkaline Phosphatase Stain Kit (Yeasen, 40749ES60) according to the manufacturer's instructions, and iPS reprogramming efficiencies were determined as frequencies of alkaline phosphatase colonies relative to input cell numbers.

Isolation of Sertoli, Leydig, and spermatogenic cells

Various testicular cell types were isolated from the whole-mouse testis using rigorous double enzymatic digestion with fraction enrichment on a Percoll (Sigma) gradient or a discontinuous BSA density gradient as described previously (53, 54). In brief, testes were collected from 8-week-old mice. Leydig cells were separated from collagenase-treated decapsulated testes by gravity sedimentation through a Percoll cushion. The dispersed seminiferous tubules were then digested with trypsin and DNase I to single-cell suspensions. Next, Sertoli cells were separated from germ cells by filtration through a 40-μm cell strainer and by adhesion to lectin-coated culture plates. Different populations of germ cells were separated by using a manually prepared 0.5–5% discontinuous BSA density gradient for velocity sedimentation sediment. After sedimentation, enriched fractions of the three germ cell types (pachytene spermatocyte, round spermatid, and elongating spermatid) were manually collected. RNA of purified somatic cell and germ cell fractions was reverse-transcribed and then analyzed by a Roche Light Cycler using primers set specific to germ cell, Sertoli cell, and Leydig cell marker genes (Table S1).

Immunoprecipitation

IP analysis was performed as described previously (8, 10). Briefly, cells were lysed and centrifuged. The supernatant was incubated with appropriate primary antibodies and protein A/G–Sepharose overnight at 4 °C. After they were washed three times with buffer containing 500 mM NaCl, immunoprecipitates were boiled with 5× loading buffer for 5 min and then subjected to Western blotting using the appropriate primary and second antibodies. All of the antibodies used in this study are listed in Table S2.

ChIP

ChIP analysis was performed as described previously (8, 10). Briefly, ESCs were cross-linked in 1% fresh formaldehyde solution followed by quenching with 0.125 M glycine. To produce chromatin fragments of 200–1000 bp, nuclear extracts were prepared in lysis buffer and sonicated using the Bioruptor (Diagenode). For immunoprecipitation, chromatin solution was mixed with appropriate antibodies and protein A/G–Sepharose beads in ChIP dilution buffer, rotated overnight at 4 °C. After they were washed twice by low-salt buffer and high-salt buffer, respectively, immunocomplexes were eluted from beads. The cross-linking of immunocomplexes was reversed, and the DNAs were purified using a DNAgel extraction kit (Axygen). Quantitative PCRs were performed using PowerUp™ SYBR Green Master Mix (Thermo Fisher Scientific) on a Roche Light Cycler. The percentage of input was calculated as $2^{-\Delta Ct}$, where $\Delta Ct = Ct(\text{CHIP}) - Ct(\text{input})$. ChIP primers are listed in Table S1.

Data availability

The RNA-Seq data are located in the Gene Expression Omnibus under accession number GSE143206.

Acknowledgments—We thank Ting Su for crucial assistance with RNA-Seq analysis. We are indebted to Drs Yun Shi and Zhaoyu Lin for helpful suggestions and for kindly providing reagents. We thank members of our laboratory for helpful discussion.

Author contributions—M. L. data curation; M. L. software; M. L., Y. Z., F. X., S. L., and J. Q. formal analysis; M. L. and J. Q. validation; M. L., Y. Z., F. X., S. L., and J. Q. methodology; M. L. and J. Q. writing-original draft; Y. X., Q. J., and J. Q. supervision; Y. X., Q. J., and J. Q. investigation; Y. X. and J. Q. project administration; J. Q. conceptualization; J. Q. resources; J. Q. funding acquisition; J. Q. writing-review and editing.

Funding and additional information—This work was supported by National Natural Science Foundation of China Grants 31671532 and 31970810 (to J. Q.).

Conflict of interest—The authors declare that they have no conflicts of interest with the contents of this article.

Abbreviations—The abbreviations used are: PcG, polycomb group; ESC, embryonic stem cell; PRC1, polycomb repressive complex 1; PRC2, polycomb repressive complex 2; IP, immunoprecipitation; sgRNA, single guide RNA; H2AK119ub1, monoubiquitination of lysine 119 in histone H2A; H3K27me3, trimethylation of lysine 27 on histone H3; H3K9me1/2, mono- and dimethylation of histone H3 lysine 9; qRT-PCR, quantitative RT-PCR; H&E, hematoxylin and eosin; GO, gene ontology; MEF, mouse embryo fibroblast; GST, GSH S-transferase; KO, knockout; GLP, G9a-like protein; HDAC, histone deacetylase.

References

1. Simon, J. A., and Kingston, R. E. (2009) Mechanisms of polycomb gene silencing: knowns and unknowns. *Nat. Rev. Mol. Cell Biol.* **10,** 697–708 CrossRef Medline
2. Di Croce, L., and Helin, K. (2013) Transcriptional regulation by Polycomb group proteins. *Nat. Struct. Mol. Biol.* **20,** 1147–1155 CrossRef Medline
3. Brand, M., Nakka, K., Zhu, J., and Dilworth, F. J. (2019) Polycomb/trithorax antagonism: cellular memory in stem cell fate and function. *Cell Stem Cell* **24,** 518–533 CrossRef Medline
4. Margueron, R., and Reinberg, D. (2011) The Polycomb complex PRC2 and its mark in life. *Nature* **469,** 343–349 CrossRef Medline
5. Turner, S. A., and Bracken, A. P. (2013) A "complex" issue: deciphering the role of variant PRC1 in ESCs. *Cell Stem Cell* **12,** 145–146 CrossRef Medline
6. Gao, Z., Zhang, J., Bonasio, R., Strino, F., Sawai, A., Parisi, F., Kluger, Y., and Reinberg, D. (2012) PCGF homologs, CBX proteins, and RYBP define functionally distinct PRC1 family complexes. *Mol. Cell* **45,** 344–356 CrossRef Medline
7. Ogawa, H., Ishiguro, K., Gaubatz, S., Livingston, D. M., and Nakatani, Y. (2002) A complex with chromatin modifiers that occupies E2F- and Myc-responsive genes in G0 cells. *Science* **296,** 1132–1136 CrossRef Medline
8. Qin, J., Whyte, W. A., Anderssen, E., Apostolou, E., Chen, H. H., Akbarian, S., Bronson, R. T., Hochedlinger, K., Ramaswamy, S., Young, R. A., and Hock, H. (2012) The polycomb group protein L3mbtl2 assembles an atypical PRC1-family complex that is essential in pluripotent stem cells and early development. *Cell Stem Cell* **11,** 319–332 CrossRef Medline
9. Trojer, P., Cao, A. R., Gao, Z., Li, Y., Zhang, J., Xu, X., Li, G., Losson, R., Erdjument-Bromage, H., Tempst, P., Farnham, P. J., and Reinberg, D. (2011) L3MBTL2 protein acts in concert with PcG protein-mediated monoubiquitination of H2A to establish a repressive chromatin structure. *Mol. Cell* **42,** 438–450 CrossRef Medline
10. Zhao, W., Tong, H., Huang, Y., Yan, Y., Teng, H., Xia, Y., Jiang, Q., and Qin, J. (2017) Essential role for polycomb group protein Pcgf6 in embryonic stem cell maintenance and a noncanonical polycomb repressive complex 1 (PRC1) integrity. *J. Biol. Chem.* **292,** 2773–2784 CrossRef Medline
11. Zdzieblo, D., Li, X., Lin, Q., Zenke, M., Illich, D. J., Becker, M., and Müller, A. M. (2014) Pcgf6, a polycomb group protein, regulates mesodermal lineage differentiation in murine ESCs and functions in iPS reprogramming. *Stem Cells* **32,** 3112–3125 CrossRef Medline
12. Endoh, M., Endo, T. A., Shinga, J., Hayashi, K., Farcas, A., Ma, K. W., Ito, S., Sharif, J., Endoh, T., Onaga, N., Nakayama, M., Ishikura, T., Masui, O., Kessler, B. M., Suda, T., *et al.* (2017) PCGF6-PRC1 suppresses premature differentiation of mouse embryonic stem cells by regulating germ cell-related genes. *eLife* **6** CrossRef Medline
13. Hu, G., Kim, J., Xu, Q., Leng, Y., Orkin, S. H., and Elledge, S. J. (2009) A genome-wide RNAi screen identifies a new transcriptional module required for self-renewal. *Genes Dev.* **23,** 837–848 CrossRef Medline
14. Matzuk, M. M., and Lamb, D. J. (2002) Genetic dissection of mammalian fertility pathways. *Nat. Cell Biol.* **4,** s41–s49 CrossRef Medline
15. Simpson, A. J., Caballero, O. L., Jungbluth, A., Chen, Y. T., and Old, L. J. (2005) Cancer/testis antigens, gametogenesis and cancer. *Nat. Rev. Cancer* **5,** 615–625 CrossRef Medline
16. Akasaka, T., Takahashi, N., Suzuki, M., Koseki, H., Bodmer, R., and Koga, H. (2002) MBLR, a new RING finger protein resembling mammalian Polycomb gene products, is regulated by cell cycle-dependent phosphorylation. *Genes Cells* **7,** 835–850 CrossRef Medline
17. Maeda, I., Okamura, D., Tokitake, Y., Ikeda, M., Kawaguchi, H., Mise, N., Abe, K., Noce, T., Okuda, A., and Matsui, Y. (2013) Max is a repressor of germ cell-related gene expression in mouse embryonic stem cells. *Nat. Commun.* **4,** 1754 CrossRef Medline
18. Pohlers, M., Truss, M., Frede, U., Scholz, A., Strehle, M., Kuban, R. J., Hoffmann, B., Morkel, M., Birchmeier, C., and Hagemeier, C. (2005) A role for E2F6 in the restriction of male-germ-cell-specific gene expression. *Curr. Biol.* **15,** 1051–1057 CrossRef Medline
19. Choi, H., Han, C., Jin, S., Kwon, J. T., Kim, J., Jeong, J., Kim, J., Ham, S., Jeon, S., Yoo, Y. J., and Cho, C. (2015) Reduced fertility and altered

epididymal and sperm integrity in mice lacking ADAM7. *Biol. Reprod.* **93,** 70 CrossRef Medline
20. Da Ros, V. G., Maldera, J. A., Willis, W. D., Cohen, D. J., Goulding, E. H., Gelman, D. M., Rubinstein, M., Eddy, E. M., and Cuasnicu, P. S. (2008) Impaired sperm fertilizing ability in mice lacking cysteine-rich secretory protein 1 (CRISP1). *Dev. Biol.* **320,** 12–18 CrossRef Medline
21. Westmuckett, A. D., Nguyen, E. B., Herlea-Pana, O. M., Alvau, A., Salicioni, A. M., and Moore, K. L. (2014) Impaired sperm maturation in RNASE9 knockout mice. *Biol. Reprod.* **90,** 120 CrossRef Medline
22. Lin, M. H., Lee, R. K., Hwu, Y. M., Lu, C. H., Chu, S. L., Chen, Y. J., Chang, W. C., and Li, S. H. (2008) SPINKL, a Kazal-type serine protease inhibitor-like protein purified from mouse seminal vesicle fluid, is able to inhibit sperm capacitation. *Reproduction* **136,** 559–571 CrossRef Medline
23. Jalkanen, J., Kotimäki, M., Huhtaniemi, I., and Poutanen, M. (2006) Novel epididymal protease inhibitors with Kazal or WAP family domain. *Biochem. Biophys. Res. Commun.* **349,** 245–254 CrossRef Medline
24. Jeong, J., Lee, B., Kim, J., Kim, J., Hong, S. H., Kim, D., Choi, S., Cho, B. N., and Cho, C. (2019) Expressional and functional analyses of epididymal SPINKs in mice. *Gene Expr. Patterns* **31,** 18–25 CrossRef Medline
25. Li, S. H., Lee, R. K., Hsiao, Y. L., and Chen, Y. H. (2005) Demonstration of a glycoprotein derived from the Ceacam10 gene in mouse seminal vesicle secretions. *Biol. Reprod.* **73,** 546–553 CrossRef Medline
26. Gaubatz, S., Wood, J. G., and Livingston, D. M. (1998) Unusual proliferation arrest and transcriptional control properties of a newly discovered E2F family member, E2F-6. *Proc. Natl. Acad. Sci. U.S.A.* **95,** 9190–9195 CrossRef Medline
27. Hurlin, P. J., Steingrìmsson, E., Copeland, N. G., Jenkins, N. A., and Eisenman, R. N. (1999) Mga, a dual-specificity transcription factor that interacts with Max and contains a T-domain DNA-binding motif. *EMBO J.* **18,** 7019–7028 CrossRef Medline
28. Takahashi, K., and Yamanaka, S. (2006) Induction of pluripotent stem cells from mouse embryonic and adult fibroblast cultures by defined factors. *Cell* **126,** 663–676 CrossRef Medline
29. Fuks, F. (2005) DNA methylation and histone modifications: teaming up to silence genes. *Curr. Opin. Genet. Dev.* **15,** 490–495 CrossRef Medline
30. Fouse, S. D., Shen, Y., Pellegrini, M., Cole, S., Meissner, A., Van Neste, L., Jaenisch, R., and Fan, G. (2008) Promoter CpG methylation contributes to ES cell gene regulation in parallel with Oct4/Nanog, PcG complex, and histone H3 K4/K27 trimethylation. *Cell Stem Cell* **2,** 160–169 CrossRef Medline
31. Cong, L., Ran, F. A., Cox, D., Lin, S., Barretto, R., Habib, N., Hsu, P. D., Wu, X., Jiang, W., Marraffini, L. A., and Zhang, F. (2013) Multiplex genome engineering using CRISPR/Cas systems. *Science* **339,** 819–823 CrossRef Medline
32. Mali, P., Yang, L., Esvelt, K. M., Aach, J., Guell, M., DiCarlo, J. E., Norville, J. E., and Church, G. M. (2013) RNA-guided human genome engineering via Cas9. *Science* **339,** 823–826 CrossRef Medline
33. Ran, F. A., Hsu, P. D., Wright, J., Agarwala, V., Scott, D. A., and Zhang, F. (2013) Genome engineering using the CRISPR-Cas9 system. *Nat. Protoc.* **8,** 2281–2308 CrossRef Medline
34. Tachibana, M., Ueda, J., Fukuda, M., Takeda, N., Ohta, T., Iwanari, H., Sakihama, T., Kodama, T., Hamakubo, T., and Shinkai, Y. (2005) Histone methyltransferases G9a and GLP form heteromeric complexes and are both crucial for methylation of euchromatin at H3-K9. *Genes Dev.* **19,** 815–826 CrossRef Medline
35. Rice, J. C., Briggs, S. D., Ueberheide, B., Barber, C. M., Shabanowitz, J., Hunt, D. F., Shinkai, Y., and Allis, C. D. (2003) Histone methyltransferases direct different degrees of methylation to define distinct chromatin domains. *Mol. Cell* **12,** 1591–1598 CrossRef Medline
36. Dovey, O. M., Foster, C. T., and Cowley, S. M. (2010) Histone deacetylase 1 (HDAC1), but not HDAC2, controls embryonic stem cell differentiation. *Proc. Natl. Acad. Sci. U.S.A.* **107,** 8242–8247 CrossRef Medline
37. Huang, Y., Zhao, W., Wang, C., Zhu, Y., Liu, M., Tong, H., Xia, Y., Jiang, Q., and Qin, J. (2018) Combinatorial control of recruitment of a variant PRC1.6 complex in embryonic stem cells. *Cell Rep.* **22,** 3032–3043 CrossRef Medline
38. Fursova, N. A., Blackledge, N. P., Nakayama, M., Ito, S., Koseki, Y., Farcas, A. M., King, H. W., Koseki, H., and Klose, R. J. (2019) Synergy between variant PRC1 complexes defines polycomb-mediated gene repression. *Mol. Cell* **74,** 1020–1036.e8 CrossRef Medline
39. Boulias, K., and Talianidis, I. (2004) Functional role of G9a-induced histone methylation in small heterodimer partner-mediated transcriptional repression. *Nucleic Acids Res.* **32,** 6096–6103 CrossRef Medline
40. Gyory, I., Wu, J., Fejér, G., Seto, E., and Wright, K. L. (2004) PRDI-BF1 recruits the histone H3 methyltransferase G9a in transcriptional silencing. *Nat. Immunol.* **5,** 299–308 CrossRef Medline
41. Nishio, H., and Walsh, M. J. (2004) CCAAT displacement protein/cut homolog recruits G9a histone lysine methyltransferase to repress transcription. *Proc. Natl. Acad. Sci. U.S.A.* **101,** 11257–11262 CrossRef Medline
42. Duan, Z., Zarebski, A., Montoya-Durango, D., Grimes, H. L., and Horwitz, M. (2005) Gfi1 coordinates epigenetic repression of p21Cip/WAF1 by recruitment of histone lysine methyltransferase G9a and histone deacetylase 1. *Mol. Cell. Biol.* **25,** 10338–10351 CrossRef Medline
43. Suzuki, A., Hirasaki, M., Hishida, T., Wu, J., Okamura, D., Ueda, A., Nishimoto, M., Nakachi, Y., Mizuno, Y., Okazaki, Y., Matsui, Y., Izpisua Belmonte, J. C., and Okuda, A. (2016) Loss of MAX results in meiotic entry in mouse embryonic and germline stem cells. *Nat. Commun.* **7,** 11056 CrossRef Medline
44. Yokobayashi, S., Liang, C. Y., Kohler, H., Nestorov, P., Liu, Z., Vidal, M., van Lohuizen, M., Roloff, T. C., and Peters, A. H. (2013) PRC1 coordinates timing of sexual differentiation of female primordial germ cells. *Nature* **495,** 236–240 CrossRef Medline
45. Cohen, I., Zhao, D., Bar, C., Valdes, V. J., Dauber-Decker, K. L., Nguyen, M. B., Nakayama, M., Rendl, M., Bickmore, W. A., Koseki, H., Zheng, D., and Ezhkova, E. (2018) PRC1 fine-tunes gene repression and activation to safeguard skin development and stem cell specification. *Cell Stem Cell* **22,** 726–739.e7 CrossRef Medline
46. Zhao, W., Huang, Y., Zhang, J., Liu, M., Ji, H., Wang, C., Cao, N., Li, C., Xia, Y., Jiang, Q., and Qin, J. (2017) Polycomb group RING finger proteins 3/5 activate transcription via an interaction with the pluripotency factor Tex10 in embryonic stem cells. *J. Biol. Chem.* **292,** 21527–21537 CrossRef Medline
47. van den Boom, V., Maat, H., Geugien, M., Rodríguez López, A., Sotoca, A. M., Jaques, J., Brouwers-Vos, A. Z., Fusetti, F., Groen, R. W., Yuan, H., Martens, A. C., Stunnenberg, H. G., Vellenga, E., Martens, J. H., and Schuringa, J. J. (2016) Non-canonical PRC1.1 targets active genes independent of H3K27me3 and is essential for leukemogenesis. *Cell Rep.* **14,** 332–346 CrossRef Medline
48. Meng, C., Liao, J., Zhao, D., Huang, H., Qin, J., Lee, T. L., Chen, D., Chan, W. Y., and Xia, Y. (2019) L3MBTL2 regulates chromatin remodeling during spermatogenesis. *Cell Death Differ.* **26,** 2194–2207 CrossRef Medline
49. Harris, T., Marquez, B., Suarez, S., and Schimenti, J. (2007) Sperm motility defects and infertility in male mice with a mutation in Nsun7, a member of the sun domain-containing family of putative RNA methyltransferases1. *Biol. Reprod.* **77,** 376–382 CrossRef Medline
50. Sapiro, R., Kostetskii, I., Olds-Clarke, P., Gerton, G. L., Radice, G. L., and Strauss Iii, J. F. (2002) Male infertility, impaired sperm motility, and hydrocephalus in mice deficient in sperm-associated antigen 6. *Mol. Cell Biol.* **22,** 6298–6305 CrossRef Medline
51. Goodson, S. G., Zhang, Z., Tsuruta, J. K., Wang, W., and O'Brien, D. A. (2011) Classification of mouse sperm motility patterns using an automated multiclass support vector machines model. *Biol. Reprod.* **84,** 1207–1215 CrossRef Medline
52. Li, L. C., and Dahiya, R. (2002) MethPrimer: designing primers for methylation PCRs. *Bioinformatics* **18,** 1427–1431 CrossRef Medline
53. Chang, Y. F., Lee-Chang, J. S., Panneerdoss, S., MacLean, J. A., 2nd, and Rao, M. K. (2011) Isolation of Sertoli, Leydig, and spermatogenic cells from the mouse testis. *BioTechniques* **51,** 341–344 CrossRef Medline
54. Da Ros, M., Lehtiniemi, T., Olotu, O., Meikar, O., and Kotaja, N. (2019) Enrichment of pachytene spermatocytes and spermatids from mouse testes using standard laboratory equipment. *J. Vis. Exp.* CrossRef Medline